

AD-A094 753

TECHNICAL  
LIBRARY

AD

AD-E400 541

TECHNICAL REPORT ARPAD-TR-80001

**AXIS: A COMPUTER'S EYE VIEW OF AN X-RAY**

JOSEPH M. ARGENTO

JANUARY 1981



US ARMY ARMAMENT RESEARCH AND DEVELOPMENT COMMAND  
PRODUCT ASSURANCE DIRECTORATE  
DOVER, NEW JERSEY

APPROVED FOR PUBLIC RELEASE; DISTRIBUTION UNLIMITED.

The views, opinions, and/or findings contained in this report are those of the author and should not be construed as an official Department of the Army position, policy or decision, unless so designated by other documentation.

Destroy this report when no longer needed. Do not return to the originator.

The citation in this report of the names of commercial firms or commercially available products or services does not constitute official endorsement or approval of such commercial firms, products, or services by the US Government.



UNCLASSIFIED

SECURITY CLASSIFICATION OF THIS PAGE(When Data Entered)

The system will be installed in an ammunition plant and will be used as the film interpreter in an actual munition line. To keep up with production, ingenious use is being made of a device called an array processor. This device allows many computer operations to be accomplished simultaneously. The array processor will permit analysis of the radiographic image in about ten seconds.

This report describes the basic techniques used to analyze a radiograph and also some of the equipment that will be used in the final system.

UNCLASSIFIED

SECURITY CLASSIFICATION OF THIS PAGE(When Data Entered)

## CONTENTS

	Page
Introduction	1
Field Flattening	2
Filtering	3
Thresholding Operation	3
Defect Measurement	4
Detection of Base Separation	4
Speedup Using the Array Processor	5
Implementation	7
Distribution List	19

## TABLE

1	Timing for major processing steps (200- by 300-pixel image)	6
---	--	---

## FIGURES

1	Block diagram of proposed system for real-time automated x-ray film reader	9
2	Digitized version of a radiograph of the aft section of artillery shell	10
3	Intensity values along horizontal cursor in figure 1	11
4	Result of field flattening with a three-strip, fourth-order polynomial	12
5	Intensity values (along horizontal cursor in fig. 1) after field flattening	13
6	Result of low-pass filtering using a 3- by 3-pixel moving-window average	14
7	Intensity values after low-pass filtering	15
8	Histogram and cumulative histogram used to obtain threshold setting	16
9	Binary image showing pixel's exceeding local thresholds	17

## INTRODUCTION

The objective of the AXIS (Automatic X-Ray Inspection System) computer program is to develop a system capable of automatically examining film radiographs of high explosive shells and making accept/reject decisions based on the presence or absence of certain classes of defects in the explosive region of the shell. Among the defect classes are small and large cavities, cracks, pipes, annular rings, foreign inclusions, regions of high porosity, and base separation. The defect indications have low contrast against a high contrast background, and some of them have dimensions comparable to the grain size of the film.

Techniques to identify and measure these defects have been developed and demonstrated on radiographs of 105-mm M1 artillery shells using a general purpose digital image processing system at the Lockheed Palo Alto Research Laboratory. More recently, a speedup in running time by some 350 times has been achieved through the use of an array processor, so the design goal of 10 seconds per shell can now be approached. A proposed configuration for a prototype system has been established, and work is progressing on extending the techniques to include the M456 antitank rounds which have a more complicated internal structure than the M1 shells.

The equipment configuration proposed for implementing the techniques at the required speeds is shown in figure 1. The limiting blocks in the diagram are the scanner-integrator for image quality and the array processor for computational speed. Experiments indicate that the use of a high resolution 1.5-inch vidicon camera, followed by logarithmic digitization and nine frames of digital integration, can reduce the entire TV contribution to less than 0.0060. Thus, the system can provide sufficient image quality for successful operation of the detection algorithms.

The five main categories of processing algorithms are:

1. Field flattening to remove the intensity trend using polynomial fitting.
2. High and low pass filtering for noise removal and for enhancement of certain defects.
3. Variable threshold setting based on histogram analysis used to separate flaws from noise.
4. Measurement of the maximum width, maximum length, and orientation of defects.

## 5. Detection of base separation.

This system has been designed to replace the skilled human inspector. When implemented, it will detect and measure defects automatically and quicker than can be done by the inspector.

### FIELD FLATTENING

The image density is sampled at 500- $\mu\text{m}$  intervals and digitized to 512 levels to form a 200- by 300-picture element (pixel) array. The result for a typical radiograph is shown in figure 2. Large density variations occur within the charge region due to shell geometry (e.g., casing diameter and thickness). Figure 3 shows the intensity variation along the row designated by the horizontal cursor in figure 2. These systematic intensity variations are large compared with intensity changes caused by flaws and, therefore, must be removed before the flaws can be detected. The intensity variation with horizontal distance is much better behaved (in the sense of being approximated by a low-order polynomial) than in the vertical direction. For this reason, the field flattening algorithm takes its input one horizontal row at a time, fits the intensity variation in the charge region with a polynomial, subtracts the estimated intensity from the actual intensity, and displays the difference (i.e., the field flattened image).

Much effort has been devoted to improving field flattening techniques because residual trends, which remain after field flattening, determine the smallest flaws which can be detected. The problem is to find a method which fits the systematic variation (which is particularly difficult due to steep slope near the shell casing) without following, and thereby subtracting, the variation caused by the flaws. The technique which gives the best result is a fourth-order polynomial operating separately on strips from the first 25%, middle 50%, and last 25% of the pixels within a single line.

The result of the field flattening operation is shown in figures 4 and 5. In these figures the estimated systematic trend has been subtracted and the difference multiplied by a factor of 8. The flaws, which are apparent in these figures, could not be observed in the input images.

## FILTERING

The noise caused by film granularity and television electronics is large compared with field flattening residuals. This noise is characterized by high spatial frequency (i.e., only a small amount of correlation between adjacent pixels) and, therefore, can be reduced by spatial low-pass filtering. However, filter parameters must be chosen which reduce the noise as much as possible without significantly reducing the amplitude of variations caused by flaws. The filter chosen is a 3- by 3-pixel moving window average. The result of low-pass filtering is given in figures 6 and 7, which show that the flaws are still clearly visible and the noise is markedly reduced.

## THRESHOLDING OPERATION

Pixels within cracks, cavities, and porosities have intensity values which are lower than "normal" and pixels within foreign inclusions have intensity values which are higher than "normal" (figs. 6 and 7). However, the problem is complicated by the fact that these "normal" values, i.e., threshold values (outside of which a pixel is potentially a defect) vary throughout the charge region. The principal causes of these threshold variations are the spatial variation of the noise and residual trends left after field flattening.

To compute these spatially dependent thresholds, the charge region is divided into 25- by 25-pixel areas as shown by the grid in figure 6. The window chosen was large enough so that the statistics would not be unduly influenced by flaws, but small enough that the flaws would not vary too much within the window. Within each window of the field-flattened image, the histogram of the 625 intensity values is computed and used to determine that intensity value which is greater than the intensity of 10% of the pixels in the window.

The thresholding operation takes as its inputs the filtered, field-flattened image and the position-dependent threshold values and produces, as output, an image in which all pixels having intensity less than the lower threshold are marked with the value 501, and those above the upper threshold are given the values 502. The Defect Processing System uses these marks to distinguish between foreign inclusions and cavities, etc. Pixels having values between these two thresholds (i.e., in the "normal" range) are given the value zero.

A typical histogram and cumulative histogram of intensities in a 25- by 25-pixel window are shown in figure 8. The threshold was set at that intensity value where the cumulative histogram reaches 10% of the pixels in the window (10% of the pixels are considered candidate defect pixels).

The region exterior to the boundary was set at a value of 511 to handle the case where the boundary cuts through portions of the window. This results in a spike in the histogram at 511 (fig. 8). In the threshold computation, consideration is given to the number of 511 marked pixels in the window by setting the cumulative number of pixel thresholds to  $0.1 [625 - N(511)]$ .

#### DEFECT MEASUREMENT

Defect pixels are grouped together based on a line adjacency criterion in which contiguous defect pixels which overlap from row to row are considered to belong to the same group. The perimeter pixels of connected groups are obtained in the host computer starting with the binary representation (fig. 9). Each group is then analyzed for maximum width, maximum length, and orientation using the array processor by means of the dot product approach.

The approach is based on the observation that if we project a line connecting two boundary pixels onto a ray of unit vectors radiating from the origin, the largest projection of the line is obtained for the unit vector most parallel to the line. Thus, we use a set of unit vectors 10 degrees apart radiating from an origin, and take the dot product of every boundary pixel of a defect group and each unit vector. We then find the maximum absolute difference (MAD) between the smallest and the largest dot product for each unit vector. The largest MAD gives the flaw orientation. The MAD on the unit vector normal to the orientation gives the maximum width. A report is printed out on defects with measurements exceeding specifications.

#### DETECTION OF BASE SEPARATION

Base separation is a defect which occurs when the explosive separates from the metal casing in the base region. This subtle flaw must be detected in the presence of a dominant intensity trend caused by the explosive-metal transition and random noise caused by film granularity and television electronics. The detection is complicated by the fact that the flaw is quite narrow, on the order

of 0.01 inch wide. For this reason, a magnified television image is used in which the pixel spacing is 125  $\mu\text{m}$  (i.e., 200 pixels per inch).

The first step is to determine the precise location of the metal case in the base region. This is accomplished by examining the intensity values within each separate column and taking as the boundary estimate that pixel having the largest derivative. These boundary estimates are refined by the use of a least square, second-order polynomial.

To reduce the film and television system noise, it is necessary to filter the data by an averaging operation. To enhance the signal caused by the flaw, this averaging should be carried out along the flaw. In the case of base separation, this direction along the flaw is known because it follows the base boundary; therefore, the intensity is averaged within "layers" parallel to the boundary determined from the second-degree polynomial. This averaging is carried out over a "sector" having a width comparable to the length of typical base separation flaws. This process is conceptually similar to a curved moving-window average one pixel high and one sector wide. In this sense the operation is analogous to the low-pass filtering operations used in the main portion of the shell.

The measured average intensities are fitted with a least square, second-degree polynomial. Points in the region where base separation can occur are not used in deriving the polynomial approximation; this prevents flaws from influencing the fit. A significant deviation between the actual and the fitted data signals the presence of a base separation.

The threshold value (beyond which the shell is rejected as having a base separation) varies from shell to shell because of changing film response. These sensitivity variations are accommodated by computing the threshold for each image based on differences between intensity values at certain prescribed points on the intensity profile. Once the threshold is computed, it is a simple matter to determine whether the deviation is too large and to print out this result on the computer-generated report.

#### SPEEDUP USING THE ARRAY PROCESSOR

The dramatic speedup achieved through the use of an array processor is indicated in table 1 where the current times for each process are compared with those required when the algorithms were programmed in Fortran on a relatively slow minicomputer.

Table 1. Timing for major processing steps  
(200- by 300-pixel image)

<u>Processing step</u>	<u>Minicomputer time (min)</u>	<u>Array processor time (sec)</u>
Field flattening	44	3 to 6
Filtering	2	1
Thresholding	9	1
Defect measurement	3	4
Base separation	1	1

The array processor (in this case, a Floating Point System AP120B) achieves its speed in four principal ways, through the use of:

1. extremely fast hardware floating point arithmetic operations
2. "pipelining" or parallel operations on serial data
3. systematic data arrangement which eliminates the need for software indexing operations

The AP120B offers an extensive library of Fortran-callable mathematical subroutines which carry out the same operation on all the elements of one or more arrays incrementing index pointers approximately and automatically. Moreover, the subroutines can be "chained" or combined to eliminate the overhead required to call each one separately from the host computer. A certain ability for thinking of problems in array or "vector" terms develops with a little experience, to the point where a surprising number of operations can be implemented efficiently in this way. Even more speedup can be achieved, should it be required, by increasing the size of the array processor's program memory, using a higher speed data memory, or programming key steps in machine language.

## IMPLEMENTATION

Once the techniques described herein have been successfully extended to the M456 antitank shell with its internal conical structure, prototype implementation can begin. In addition to the software processing steps described, hardware and software for such operations as film positioning and movement, report generation, and overall sequency and control must be designed for full implementation. It is anticipated that the resulting system will not only perform the work as well as the skilled human inspector, but will do so automatically and in a shorter time.

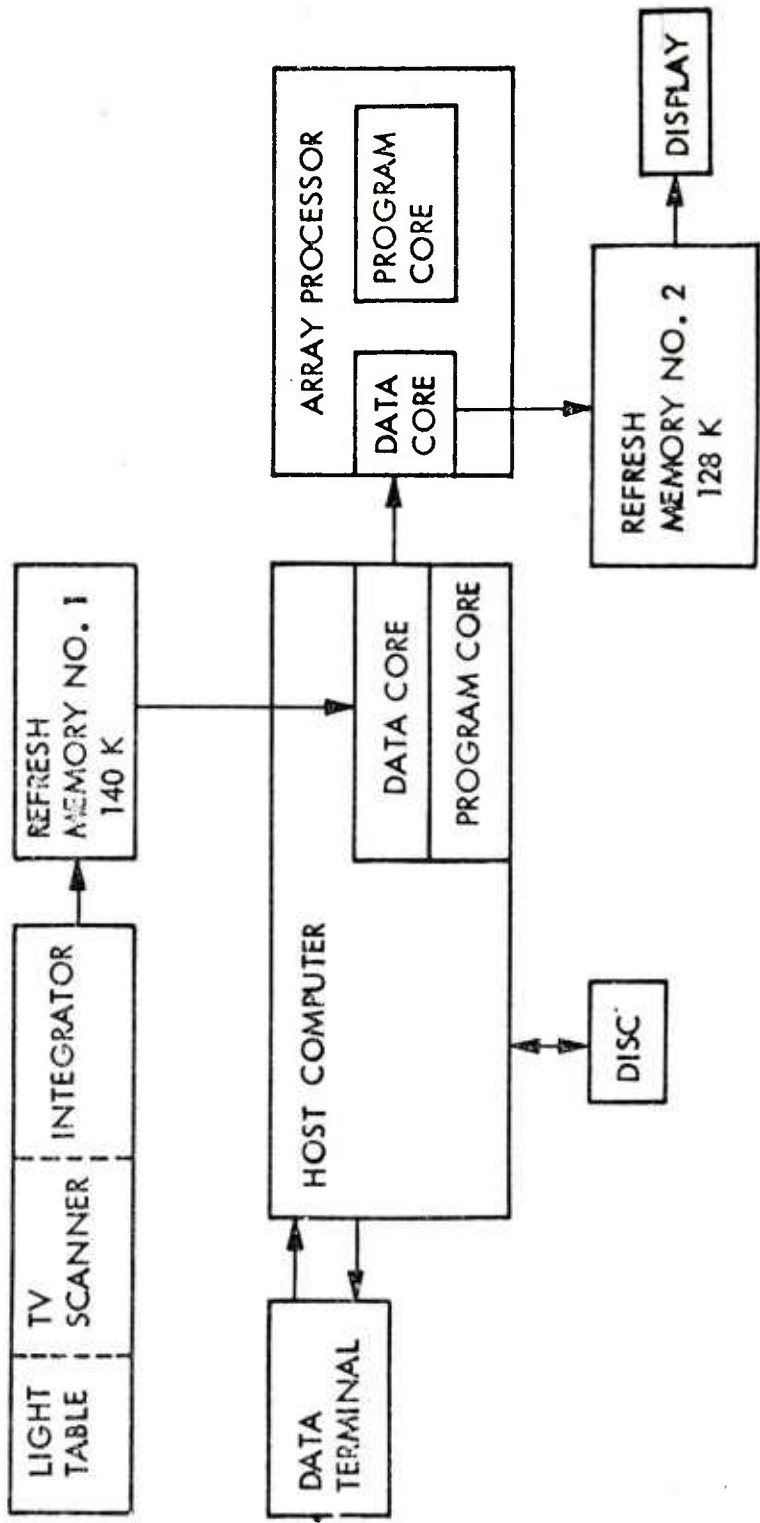


Figure 1. Block diagram of proposed system for real-time automated x-ray film reader

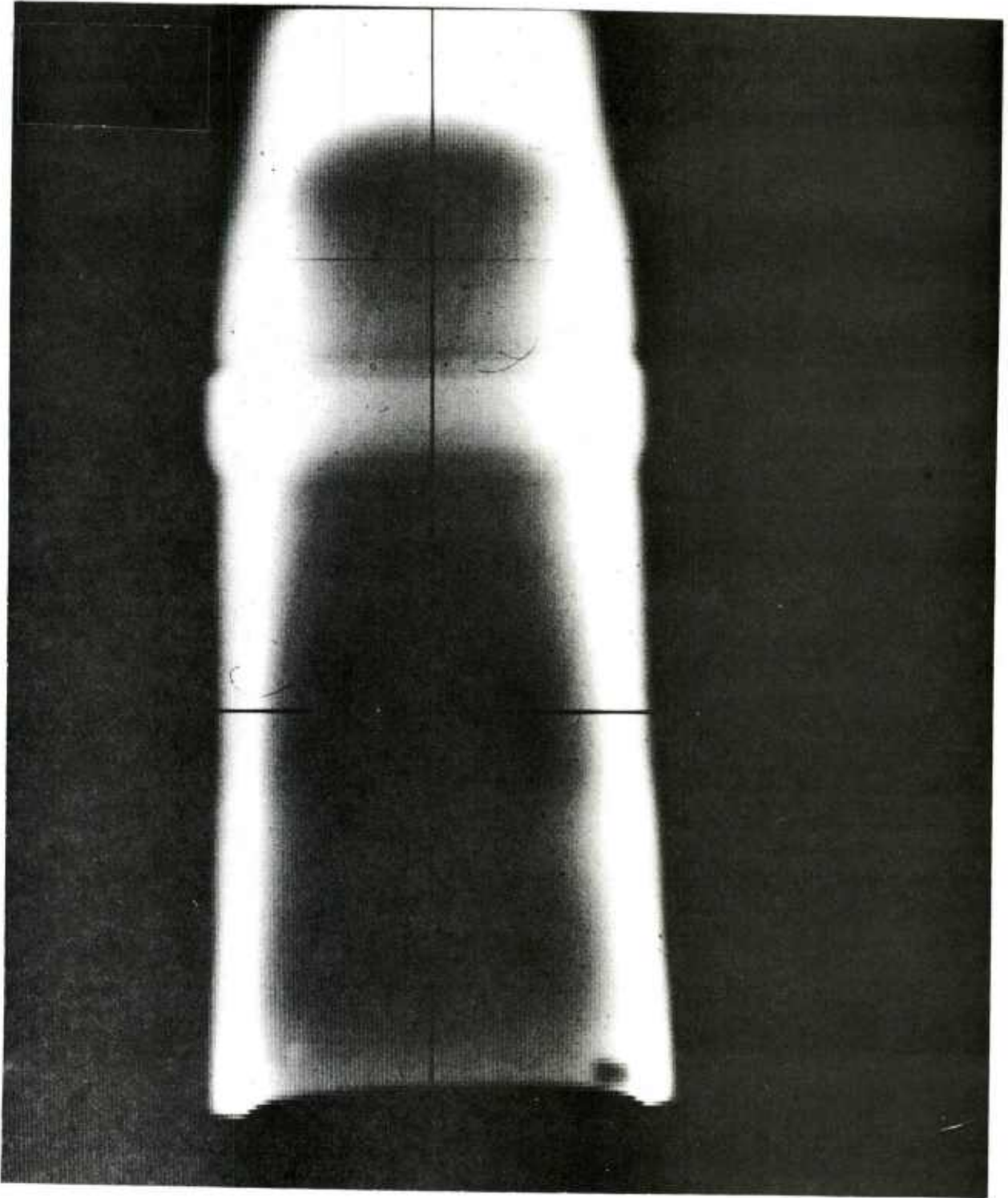


Figure 2. Digitized version of a radiograph of the aft section of artillery shell

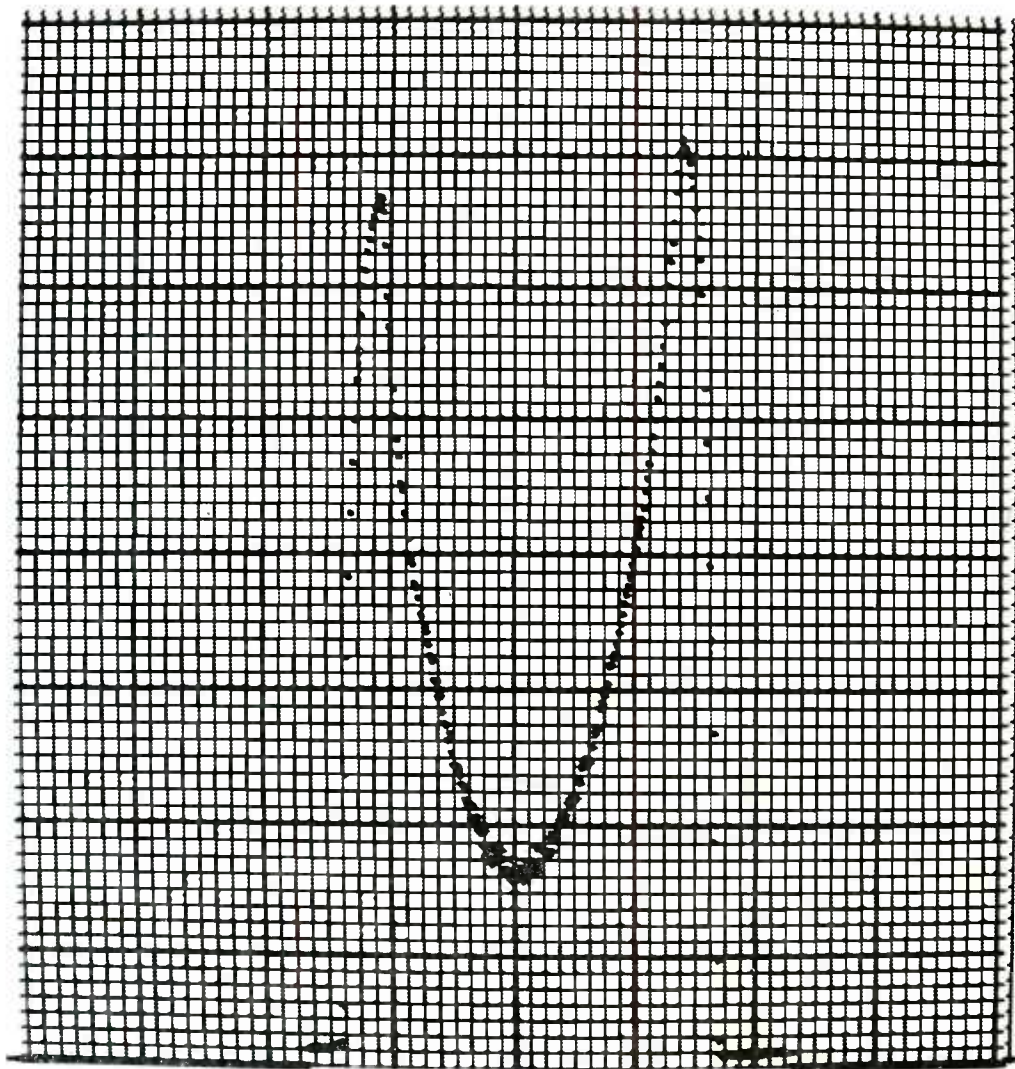


Figure 3. Intensity values along horizontal cursor in figure 1

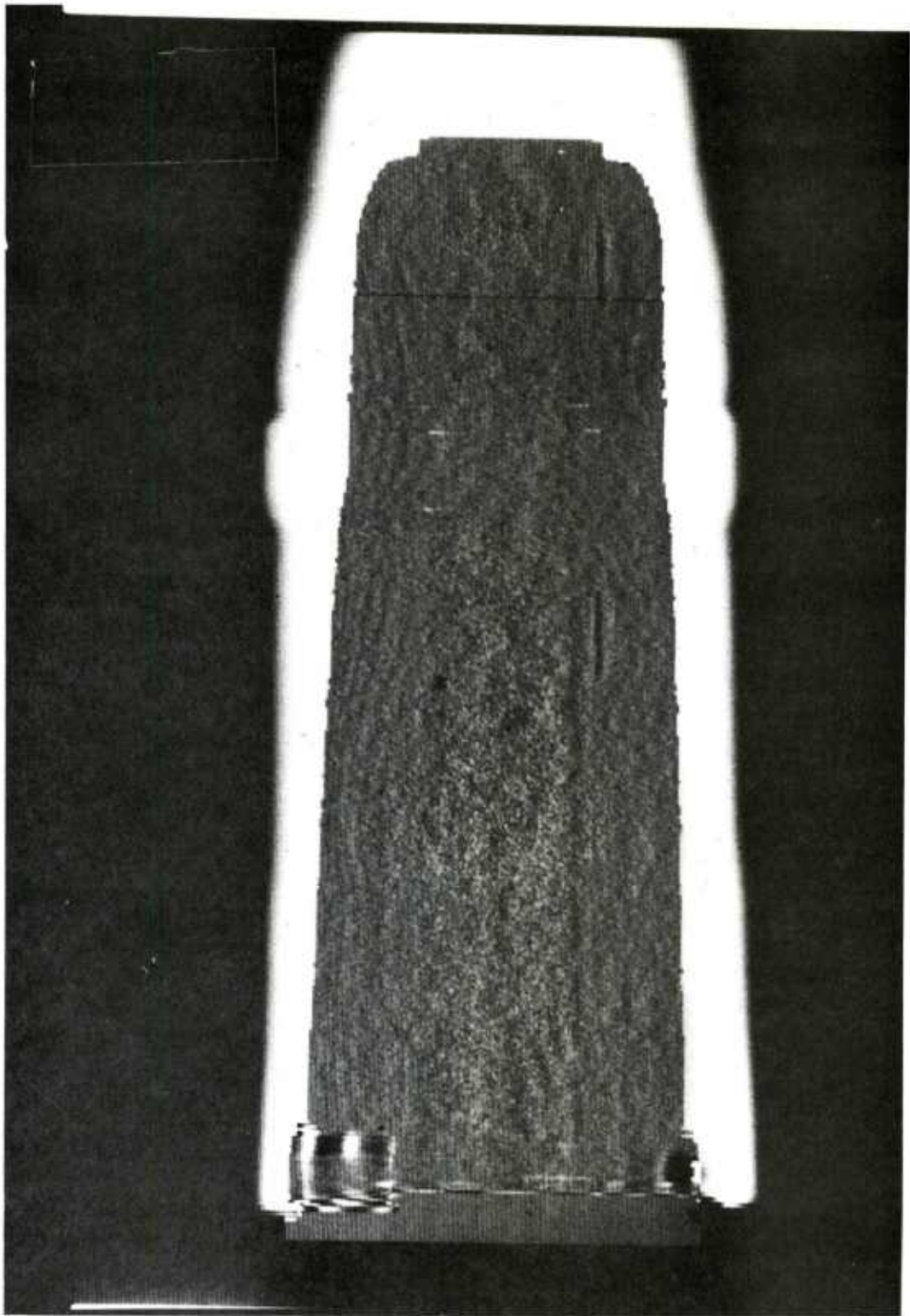


Figure 4. Result of field flattening with a three-strip, fourth-order polynomial

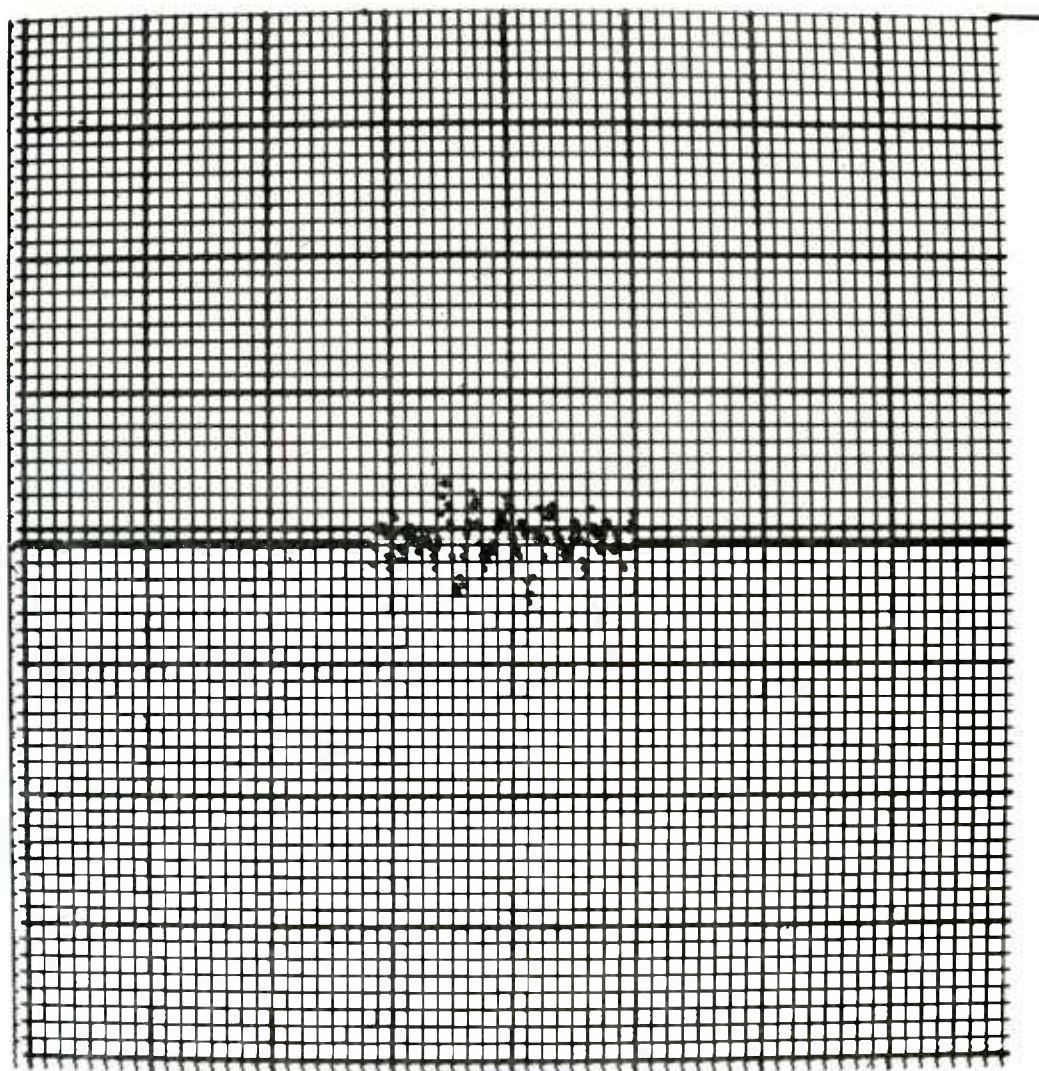


Figure 5. Intensity values (along horizontal cursor in fig. 1) after field flattening

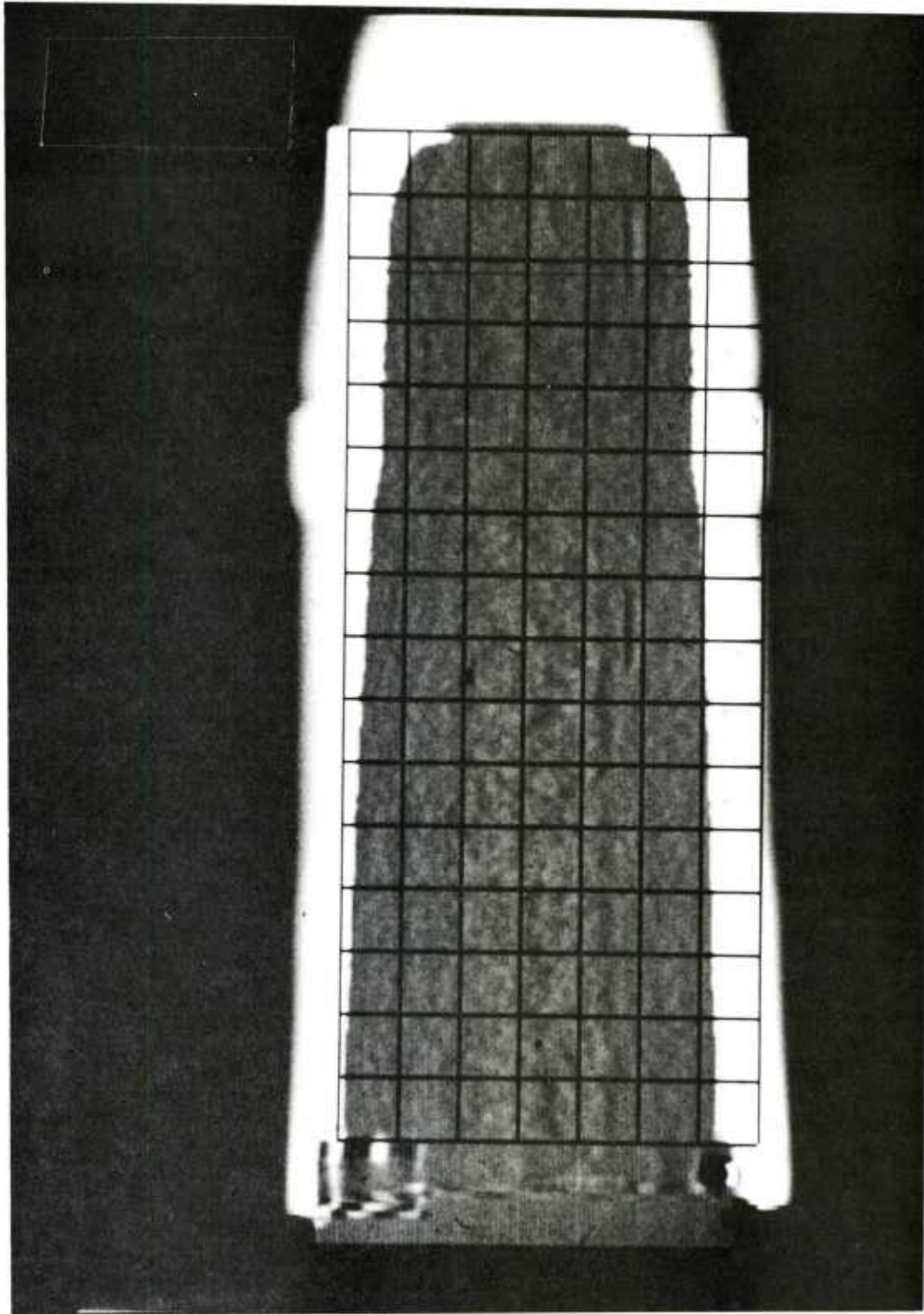


Figure 6. Result of low-pass filtering using a 3- by 3-pixel moving-window average

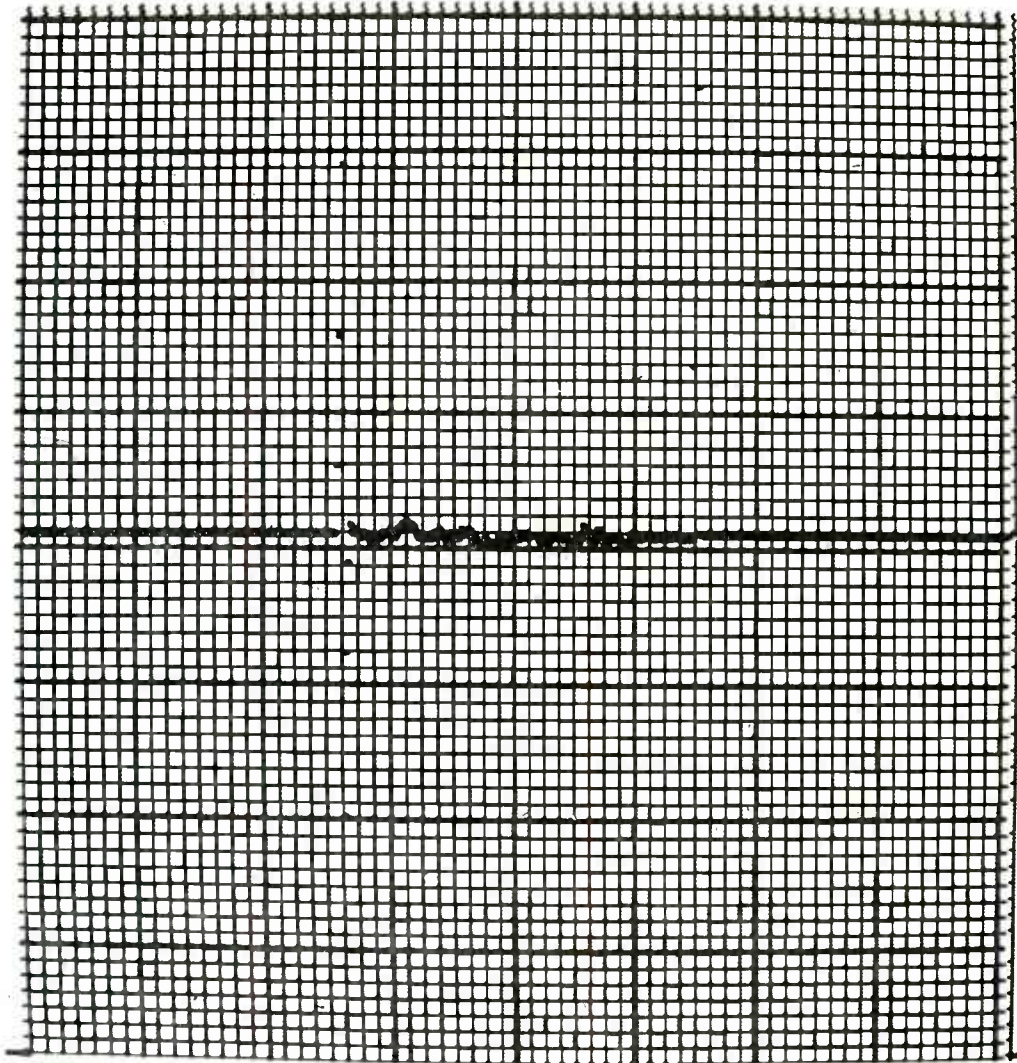
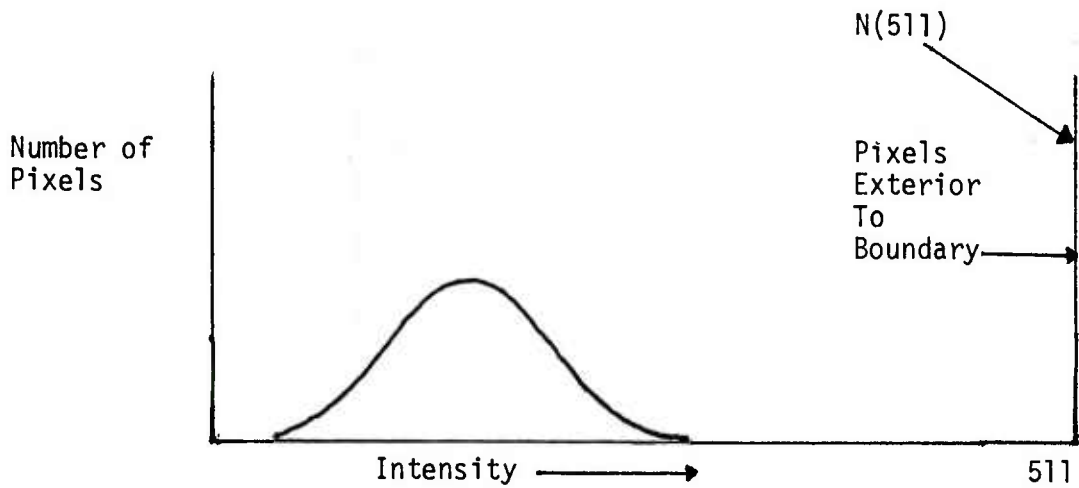
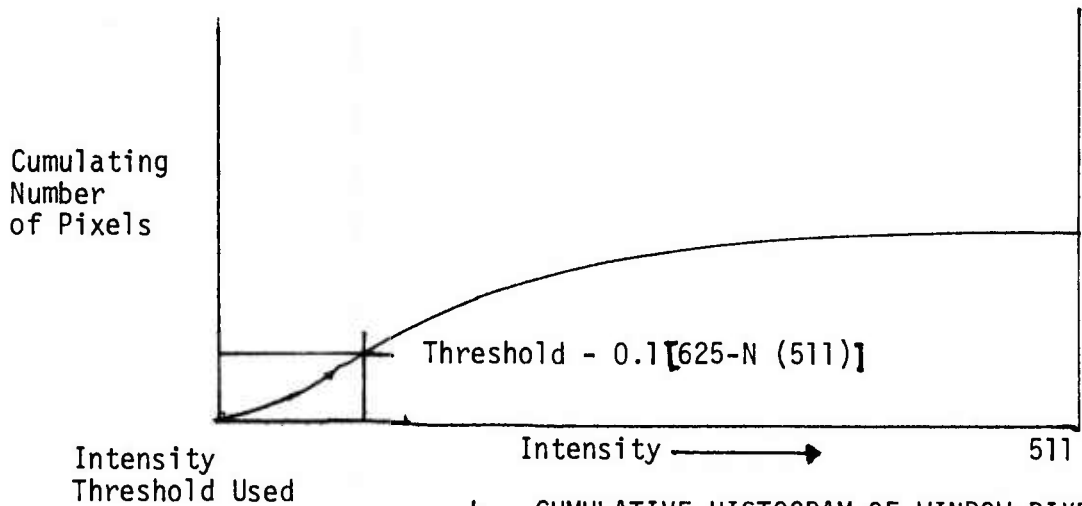


Figure 7. Intensity values after low-pass filtering



a. HISTOGRAM OF WINDOW PIXELS



b. CUMULATIVE HISTOGRAM OF WINDOW PIXELS

Figure 8. Histogram and cumulative histogram used to obtain threshold setting

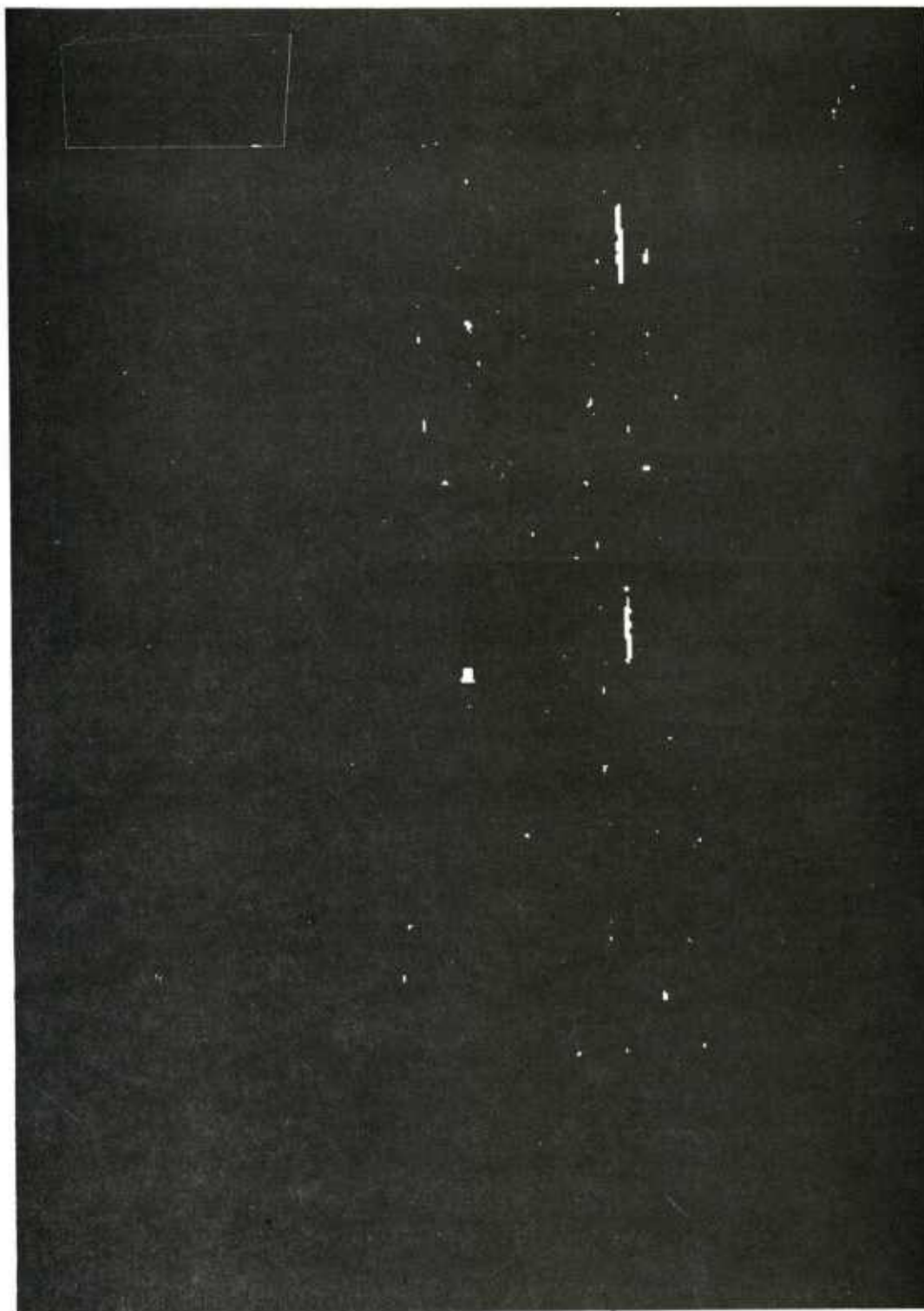


Figure 9. Binary image showing pixel's exceeding local thresholds

DISTRIBUTION LIST

Commander  
U.S. Army Armament Research and  
Development Command  
ATTN: DRDAR-QAS (10)  
DRDAR-QAR (5)  
DRDAR-QAN (5)  
DRDAR-TSS (5)  
DRDAR-GCL  
Dover, NJ 07801

Administrator  
Defense Technical Information Center  
ATTN: Accessions Division (12)  
Cameron Station  
Alexandria, VA 22314

Commander  
U.S. Army Armament Materiel  
Readiness Command  
ATTN: DRSAR-LEP-L  
Rock Island, IL 61299

Commander/Director  
Chemical Systems Laboratory  
U.S. Army Armament Research  
and Development Command  
ATTN: DRDAR-CLJ-L  
APG, Edgewood Area, MD 21010

Director  
Ballistics Research Laboratory  
U.S. Army Armament Research  
and Development Command  
ATTN: DRDAR-TSB-S  
Aberdeen Proving Ground, MD 21005

Chief  
Benet Weapons Laboratory (LCWSL)  
U.S. Army Armament Research  
and Development Command  
ATTN: DRDAR-LCB-TL  
Watervliet, NY 12189

Commander  
U.S. Army Armament Research  
and Development Command  
Weapons Systems Concept Team  
ATTN: DRDAR-ACW  
APG, Edgewood Area, MD 21010

Director  
U.S. Army Materiel Systems  
Analysis Activity  
ATTN: DRXSY-MP  
Aberdeen Proving Ground, MD 21005

Commander  
U.S. Army Munitions Production  
Base Modernization Agency  
ATTN: SARPM-PBM  
Dover, NJ 07801